

# Corrosion Behavior of Nickel-Based Alloys in Supercritical Water Oxidation Systems

D. B. Mitton,\* J.-H. Yoon, J. A. Cline, H.-S. Kim, N. Eliaz, and R. M. Latanision

*H.H. Uhlig Corrosion Laboratory, Department of Materials Science and Engineering, Massachusetts Institute of Technology, Room 8-204, Cambridge, Massachusetts 02139*

There is a need to destroy both military and civilian hazardous waste and an urgency, mandated by public concern over traditional waste handling methodologies, to identify safe and efficient alternative technologies. One very effective process for the destruction of such waste is supercritical water oxidation (SCWO). By capitalizing on the properties of water above its critical point (374 °C and 22.4 MPa for pure water), this technology provides rapid and complete oxidation with high destruction efficiencies at typical operating temperatures. Nevertheless, corrosion of the materials of fabrication is a serious concern. While Ni and Ni-based alloys are generally considered important for severe service applications, results from laboratory and pilot-scale SCWO systems presently in operation indicate that they will not withstand some aggressive feeds. Significant weight loss and localized effects, including stress corrosion cracking and dealloying, are seen in some environments. Although exotic liners such as platinum are currently promoted as a solution to aggressive conditions, some evidence suggests the potential for corrosion control by judicious feed modification. Various alloys were exposed in a SCWO system at 600 °C for 66.2 h. After exposure, samples were coated with a thick outer salt layer and an inner oxide layer. It is considered likely that, at the high supercritical temperature employed during this test, the salt was molten and contained a substantial quantity of gas. The inner oxide layer revealed the presence of numerous defects and a thickness that is proportional to the corrosion rate determined by mass loss, suggesting the oxide layer is nonprotective. Of the alloys tested, G-30 exhibited the highest corrosion resistance. Experiments in which a C-276 tube was instrumented with thermocouples and exposed to a HCl feed indicate for this simple non-salt-forming influent that there is a strong correlation between temperature and the extent and form of corrosion, with the most pronounced degradation being at high subcritical temperatures. These experiments corroborate previous results from a failure analysis for C-276, suggesting a corrosion maximum in the subcritical region.

## Background

During the Workshop on Corrosion in Supercritical Water Oxidation (SCWO) Systems held at Massachusetts Institute of Technology in 1993 the attendees recognized the potential that corrosion problems could restrict the commercialization of SCWO for aggressive waste streams. At that time, the group consensus was that a material of fabrication universally applicable to all sections of a SCWO system was extremely unlikely. While the database for the potential materials of fabrication for SCWO systems has increased significantly since then, the group consensus still holds. The corrosion of the materials of fabrication remains a serious concern, and a significant amount of research remains to be carried out to identify materials or methods to reduce degradation within all sections to an acceptable level.

There is in excess of 23 000 tons of chemical agent stockpiled at eight sites within the continental U.S. The composition and nomenclature for a number of agents are presented in Table 1.<sup>1</sup> While production was stopped in the late 1960s, some of this waste may have originated as long ago as the 1940s.<sup>2</sup> In addition to stockpiled munitions, there exists a significant, but unknown, quantity of nonstockpiled waste that also needs to be

**Table 1. Composition and Nomenclature for a Number of Chemical Agents<sup>1</sup>**

agent	composition
GB (Sarin) VX	isopropyl methylphosphonofluoridate <i>O</i> -ethyl <i>S</i> -diisopropylaminomethyl methylphosphonothiolate
HD (mustard) GF	bis(2-chloroethyl)sulfide cyclohexyl methylphosphonofluoridate
GD (Soman) GA (Tabun)	pinacolyl methylphosphonofluoridate <i>O</i> -ethyl dimethylamidophosphoryl cyanide

considered for destruction.<sup>3,4</sup> This is a growing technical challenge because of the variety and circumstances in which it is found.<sup>1,3,4</sup> The Chemical Weapons Convention (CWC), which was signed by 130 countries, seeks to eliminate chemical weapons and their production early in the new millennium.<sup>2,5</sup> To be able to accomplish this, a safe, efficient, and economical waste disposal methodology needs to be identified. While a number of traditional destruction methodologies such as landfill or incineration do currently exist, they face significant public opposition.<sup>6</sup> Further, the economics of incineration requires a relatively high concentration of waste in the feed, and the practice of permitting aqueous waste concentration by evaporation in open ponds prior to disposal is no longer acceptable.

In addition to chemical agents, there is a need for the Department of Energy (DOE) to address the clean up of in excess of 160 000 m<sup>3</sup> of mixed waste in its charge.

\* To whom correspondence should be addressed. E-mail: Bmitton@mit.edu. Phone: (617) 253-3313.

While SCWO is demonstrably capable of destroying such wastes, many of the DOE wastes contain solvents or oils that are high in chlorine or other potentially corrosive precursors (e.g., fluorine, sulfur, and tributyl phosphate). During destruction by SCWO, these can be oxidized to acidic products. In the case of chemical agents (Table 1), the oxidation of Sarin (GB) produces a mix of hydrofluoric and phosphoric acids; the oxidation of VX results in sulfuric and phosphoric acids; and finally, the oxidation of mustard agent (HD) produces hydrochloric and sulfuric acids.<sup>7</sup> Such acidic conditions may result in significant corrosion of the process unit, and in the context of the development of scaled-up systems,<sup>8-10</sup> corrosion may ultimately be the deciding factor in the commercial application of this technology.

**Characteristics and Benefits of the SCWO Process.** This is a promising technology applicable to many dilute organic wastes<sup>11-13</sup> in the range 1-20% which are not suitable for disposal by either incineration or landfill.<sup>6</sup> As the critical point is approached, the density of water changes rapidly as a function of changes in either temperature or pressure. In this regime, the density is intermediate between that of liquid water ( $1 \text{ g cm}^{-3}$ ) and low-pressure water vapor ( $<0.001 \text{ g cm}^{-3}$ ). Typically, at SCWO conditions, the water density is approximately  $0.1 \text{ g cm}^{-3}$  and, consequently, the properties of supercritical water are significantly different from those of liquid water at ambient conditions. The dielectric constant of water at 25 MPa drops from approximately 80 at room temperature to 2 at 450 °C, and the ionization constant decreases from  $10^{-14}$  at room temperature to  $10^{-23}$  at supercritical conditions. These changes result in supercritical water acting essentially as a nonpolar dense gas with solvation properties approaching those of a low-polarity organic. Under these conditions, hydrocarbons generally exhibit high solubility in supercritical water and, conversely, the solubility of inorganic salts is very low. The solubility of NaCl, for example, drops from about 37 wt % at 300 °C to only 120 ppm at 550 °C. The combination of the solvation and physical properties makes supercritical water an ideal medium for the oxidation of organics. When organic compounds and oxygen are dissolved in water above the critical point, kinetics are fast and the oxidation reaction proceeds rapidly to completion. While the products of hydrocarbon oxidation are  $\text{CO}_2$  and  $\text{H}_2\text{O}$ , heteroatoms are converted to inorganic compounds (usually acids, salts, or oxides in high oxidation states). As a result of the relatively low temperature of operation,  $\text{NO}_x$  and  $\text{SO}_2$  are not produced.<sup>11</sup> The latter may be particularly important during the destruction of explosives, which produce nitrogen oxides during incineration.<sup>14</sup>

Figure 1 presents a schematic diagram of a waste treatment system based on SCWO technology.<sup>12</sup> In this process, aqueous organic waste (1), which may be neutralized with a caustic solution (2) or have fuel (3) injected for startup, is initially pressurized from ambient to the pressure of the reaction vessel and pumped through a heat exchanger (4). This helps to bring the stream up to the desired temperature before reaching the reactor. At the head of the reactor (5), the stream is mixed with air or oxygen. In some cases, an oxidant such as hydrogen peroxide ( $\text{H}_2\text{O}_2$ ) may be utilized in preference to either air or oxygen; however, this is not economically advantageous. The reaction occurs in the top zone (6), where spontaneous oxidation of the organ-

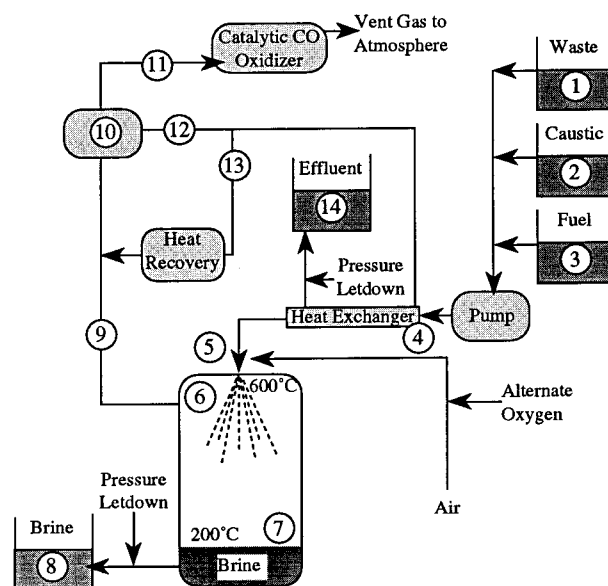


**Figure 1.** Schematic representation of a waste treatment system based on SCWO technology.

ics liberates heat and raises the temperature to levels as high as 650 °C. Organic destruction occurs quickly, with typical reactor residence times of 1 min or less. As a result of their low solubility, salts precipitate and impinge on the lower zone (7), which is at a temperature of about 200 °C. The salts may be continuously taken off as a brine (8) or removed periodically as solids. The primary effluent (9) passes out the top of the reactor into a separator (10), where the gas (11) and liquid (12) are quenched and separated. Finally, while a portion of the liquid remains in the system and is recycled (13), some is taken off as an effluent (14). Heat can be recovered from the treatment process stream and used to preheat the feed (4) or potentially to produce steam for electric power generation.<sup>11</sup>

**Corrosion Problems in SCWO Systems.** The major disadvantages of SCWO revolve around high pressure ( $P > 23 \text{ MPa}$ ), potential solids handling problems, and, for some waste streams, corrosion.<sup>11</sup> Although SCWO is technologically able to destroy hazardous wastes, the process must be carried out in a reactor capable of accommodating elevated temperatures, pressures, and degradation problems<sup>15-33</sup> that may result from aggressive feed streams.

Because high-nickel materials have traditionally been employed for severe service applications,<sup>21</sup> they have been utilized during fabrication of a number of bench-scale and pilot-plant reactors. The current database, nevertheless, suggests that these materials may not be suitable for the most aggressive "untreated" SCWO feed streams<sup>7,8,15,17,22-27</sup> because they can exhibit both significant weight loss and localized effects including pitting, stress corrosion cracking (SCC), and dealloying in such environments.

As early as 1990,<sup>29</sup> dealloying of Cr and Mo (I-625) or Cr, Mo, and W (C-276) was recognized as a potential contributor to degradation within SCWO systems. Based on effluent analysis, results suggested loss of chromium for nonchlorinated feeds, while selective dissolution of the main alloying element, Ni, was apparent for chlorinated feeds.<sup>30</sup> Corroboration was subsequently provided<sup>24,25</sup> by metallographic examination during analysis of a failed C-276 SCWO preheater tube, which, for acidic chlorinated conditions, revealed severe depletion

of Ni. Interestingly, this analysis also suggested that the most severe corrosion was associated with a high subcritical temperature<sup>25</sup> and that, at supercritical conditions, in the absence of salt precipitates, corrosion may actually be minimal for alloys such as C-276.<sup>31</sup> At supercritical temperatures for an untreated acidic chlorinated feed,<sup>32</sup> high-nickel alloys I-625, C-22, and I-686 apparently follow a general trend in which the corrosion rate decreases between 400 and 600 °C; however, a significant increase was recorded above 600 °C. Conversely, within the same temperature range, the corrosion rate of C-276 increased with increasing temperature. While one report suggests no apparent pattern in the location of localized corrosion for alloy 625,<sup>23</sup> there is significant evidence to suggest that the potential for corrosion of Ni alloys exposed to SCWO conditions is more pronounced in the high subcritical regime<sup>24–26,33</sup> and that the aggressiveness of the solution may decrease above the critical point<sup>34</sup> as a result of the presence of only nondissociated HCl and reduced solution conductivity.<sup>35</sup> Care is, however, necessary in extrapolating such behavior, because cracking has also been reported at supercritical temperatures after extended exposure times.<sup>8</sup> In addition, to some extent, the upper temperature limit for severe corrosion depends on the pressure and, thus, the density of the solution, with higher densities favoring corrosion.<sup>33</sup> While an Inconel 625 tube exposed to an aqueous feed stream containing 1800 ppm HCl without the addition of oxygen revealed only general corrosion,<sup>16</sup> a 10-fold increase in the concentration (18 000 ppm) resulted in transgranular SCC within the subcritical temperature zone (300 °C) after exposure for only 46 h. Under more complex low pH conditions, others<sup>27</sup> report both transgranular and intergranular cracking of I-625 at subcritical, but not at supercritical, temperatures. Hong has, however, previously reported observing SCC and pitting of I-625 exposed to a mixed methylene chloride/isopropyl alcohol feed neutralized with NaOH after extended times at supercritical temperatures (300 h at 580 °C).<sup>8</sup> In general, when tested in chemical agent simulant feeds, corrosion of the nickel alloys (C-22, C-276, 625, 825, and HR-160) was unacceptably high for both chlorinated and nonchlorinated simulants.<sup>7</sup> When exposed to a highly chlorinated feed at 600 °C for a short duration (66.2 h), HR-160 exhibited a reasonable performance based on weight loss data; however, in regions where the surface oxide layer was locally disrupted, severe grain boundary corrosion was apparent.<sup>19</sup> There is some evidence for a correlation between the Cr content and corrosion resistance for Ni alloys in SCWO systems.<sup>36</sup> The high Cr alloys such as G-30 ( $\approx 30\%$  Cr) exhibit a reasonable corrosion resistance.<sup>10,19,37</sup> For a maximum temperature of 350 °C, results<sup>20</sup> indicate a rate of approximately 4 mmpy (millimeters per year) for G-30 exposed to an acidic chlorinated feed.

**Potential Methodologies for Reducing Corrosion Damage.** A recognition of materials degradation as one of the central challenges to the ultimate commercialization of this technology has precipitated a number of potential methodologies for corrosion mitigation.

**(a) Corrosion-Resistant Liners and Coatings.** One potential methodology for reducing corrosion damage during the destruction of aggressive feeds would involve the use of a corrosion-resistant liner in conjunction with a pressure-bearing wall. Although some

progress has been made in circumventing corrosion problems in this way, liners have not been extensively tested in these systems and, as previously mentioned, there are conflicting reports on corrosion of basic materials. In addition, the liner materials (titanium and platinum) most frequently suggested for aggressive feed streams tend to be expensive.

**(b) Feed Modification.** One possible alternative (or addition) to the use of corrosion-resistant liners would be to adjust the feed stream chemistry such that serious degradation is minimized. It may be possible to accomplish this by reducing the chloride concentration, or by altering the pH and oxidizing conditions, such that the most favorable thermodynamics are obtained.

Sufficient dilution of an aggressive feed can potentially reduce the risk of corrosion by lowering the chloride concentration and, thus, permit processing by SCWO. The required dilution may, however, be so large as to make such a procedure economically unattractive. For example, a dilution of 1000–10 000 for wastes high in solvents such as carbon tetrachloride may be required to reduce feeds to acceptable levels.<sup>38</sup>

Although feed neutralization, with NaOH, for example, has seen some success in SCWO systems for acidic feeds, it has been carried out without a full understanding of its effect on corrosion within a system. Typically, feed neutralization involves stoichiometric quantities of neutralizer; however, there is evidence<sup>25</sup> that a limited *E*-pH region exists within which the stability of Ni, Cr, and Fe is thermodynamically favored for high subcritical conditions. Thus, the addition of the incorrect quantity of neutralizer may result in corrosion of systems fabricated from alloys containing these elements.

**(c) Reactor Design.** Over the years, a number of new or modified reactor designs have emerged. In general, these designs attempt to reduce exposure of the pressure-bearing wall to the process fluid and to limit potential problems with plugging. In its simplest form, design modification has involved the use of a liner with deionized water between the vessel wall and the liner.<sup>39</sup> More complex designs have included the dual-shell pressure-balanced vessel (DSPBV),<sup>40</sup> the transpiring wall reactor, and the reactor concept of a film-cooled coaxial hydrothermal burner (FCHB).<sup>41,42</sup> In the latter case, while the authors were initially optimistic about the design,<sup>41</sup> subsequent experiments revealed problems including corrosion of the core tube tip and coaxial tubes.<sup>42</sup>

## Recent Results

**Failure Analysis.** Figure 2 presents both a schematic representation of an experimental plug-flow reactor (PFR) and a number of micrographs of the tube cross section at selected locations within the PFR. This system is employed to study the kinetics and reaction mechanisms of the destruction of organics in supercritical water. The organic preheaters were employed to heat an aqueous methylene chloride ( $\text{CH}_2\text{Cl}_2$ ) feed solution ( $0.017\text{--}0.057\text{ mol L}^{-1}\text{ CH}_2\text{Cl}_2$ ) to the temperature of the reactor. Although isothermal conditions were maintained in the reactor (450–600 °C) during individual experiments, the preheater temperature varied from ambient at the entrance to supercritical at the exit. The alloy C-276 tubes employed as organic preheaters were approximately 250–300 cm long and had an outside diameter (o.d.) of 1.6 mm. The total time of exposure to



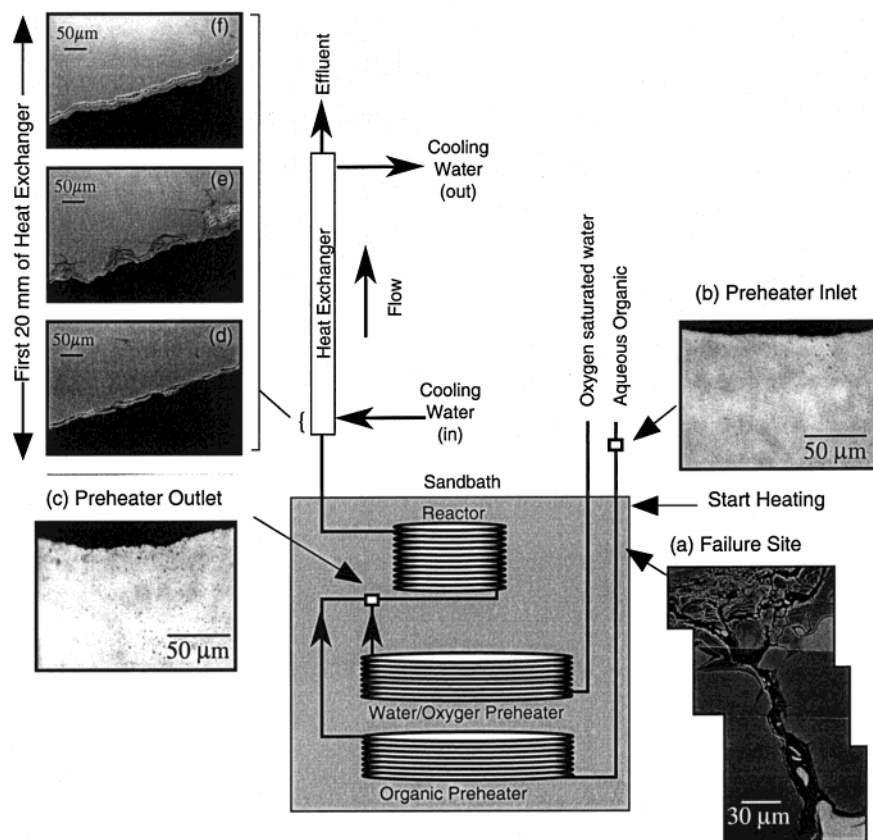


**Figure 2.** Schematic representation of an experimental PFR and a number of micrographs (a–f) of the tube cross section at selected locations within the PFR.

the feed solution prior to failure was 104 h for the first, 45 h for the second, and 56 h for the third preheater.

Ultimately, all three units failed by the development of an axial intergranular crack (Figure 2 a). In general, the inner diameter of the tube wall in the region of the failure site displayed dealloying<sup>25</sup> of Ni, Fe, and Mo and enrichment of Cr. It is significant that although different conditions (temperature, feed type, and composition) were employed during the various experiments, the three individual failures all occurred in the same general region of tube between 37.5 and 59 cm from the inlet end of the preheater. There was no appreciable corrosion either at the preheater inlet (Figure 2 b), which was at near ambient temperature, or at the preheater exit (Figure 2c), which experienced significant HCl concentrations at supercritical conditions. The exit to the preheater (Figure 2c) and inlet to the cool-down heat exchanger (Figure 2d), which are known to be at supercritical conditions, both reveal low rates of corrosion. A short distance into the cool-down heat exchanger (Figure 2e), crack development is observed. The form of corrosion observed within the cool-down heat exchanger echoes the corrosion morphology seen within the preheater, and elemental analysis indicates selective dissolution of Ni, Fe, and Mo as well as enrichment of Cr. Finally, beyond this point the corrosion rate within the cool-down heat exchanger decreases (Figure 2f) as a function of decreasing temperature.

No thermocouple was located in the vicinity of the preheater failure site. Nevertheless, because corrosion tended to be minimized within known supercritical regions, cracking was assumed to develop preferentially within a high subcritical regime.<sup>25</sup> Rapid crack development could compromise the system integrity and, thus,

foreknowledge of the probable location of maximum degradation would be important during the system design. A subsequent section of this paper deals with this in more detail.

**Correlation between Thermodynamics and Corrosion.** In general, during the failure analysis, dealloying of Ni, Mo, and Fe and enrichment of Cr were observed. We previously suggested<sup>25</sup> the potential that an  $E$ -pH region thermodynamically favorable to the stability of Ni-based alloys may be obtainable by feed modification. It was apparent from the results that there was a region of the  $E$ -pH diagram where thermodynamic conditions favored the formation of both insoluble chromium and soluble Ni, Fe, and Mo. Additionally, it became clear during that analysis that a moderate increase in pH could result in a significant change in the corrosion behavior of the C-276 alloy. It was hypothesized that an increase in pH could favor either the stability of Cr, Ni, and Fe (less oxidizing conditions) or the loss of Cr stability in conjunction with the formation of a stable Ni oxide (more oxidizing conditions).

It is important to recognize the restrictions of this type of diagram: they refer to pure, defect-free, unstressed metals in pure water. Although they reveal the reactions which are thermodynamically possible (or impossible), they do not indicate the rate at which these reactions may take place. Nevertheless, such diagrams are still able to provide valuable information.

Figure 3 presents both (a) the experimentally determined<sup>43</sup> relative concentration of Ni, Cr, and Mo in the effluent for an Inconel 625 reactor exposed to various feed pH values and (b) a combination  $E$ -pH diagram for Ni, Cr, and Mo at 300 °C.<sup>25</sup> The concentrations of

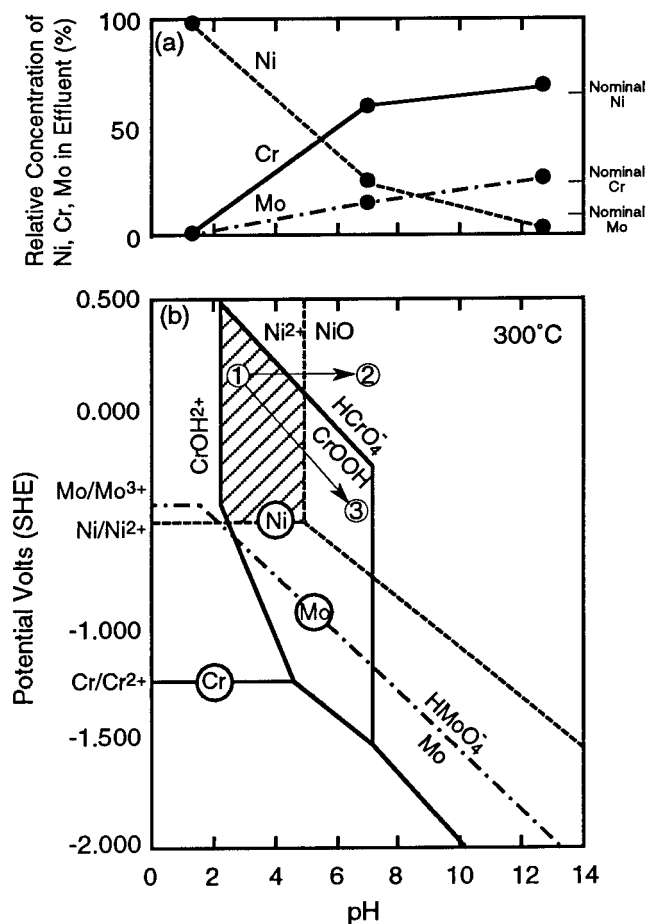


**Figure 3.** (a) Experimentally determined<sup>43</sup> relative concentrations of Ni, Cr, and Mo in the effluent for an Inconel 625 reactor exposed to various feed pH values and (b) a combination  $E$ -pH diagrams for Ni, Cr, and Mo at 300 °C.<sup>25</sup>

Ni, Cr, and Mo in the effluent were experimentally determined at three ambient pH values: 1.3, 7.0, and 12.7 at a high subcritical maximum test temperature ( $T_{\max} \approx 350$  °C) and tabulated in the literature.<sup>43</sup> Figure 3a was derived from the tabulated data and presents the relative concentration of Ni, Cr, and Mo in the effluent for an Inconel 625 reactor exposed to various feed pH values. These data have been presented in Figure 3a using the same abscissa (pH) as the  $E$ -pH diagram presented in Figure 3b. When the data are presented in this way, a number of interesting features become apparent.

**(a) Acidic Chlorinated Feed (pH 1.3).** For these conditions, while the nickel concentration in the effluent is appreciably higher than the nominal alloy value, the Cr and Mo effluent concentrations are significantly lower than the nominal values. In agreement with our previous work indicating dealloying of alloy C-276 in acidic chloride media,<sup>25</sup> these data indicate that conditions are such that Ni is unstable while Cr is stable, resulting in selective dissolution of Ni. From the  $E$ -pH diagram (Figure 3b), this suggests the probability of conditions associated with the stability of Ni<sup>2+</sup> and CrOOH (shaded region). The pH of the feed was slightly more acidic (1.3) than the soluble/insoluble Cr species line (pH  $\approx$  2). The  $E$ -pH diagram, however, represents conditions at 300 °C, while the pH of the feed was determined at ambient conditions. The metal (Ni, Cr, and Mo) loss for this experiment was approximately 1589 ppm after 15 h.

**(b) Neutral Chlorinated Feed (pH 7).** With the shift in pH from acidic to more neutral conditions, there has been a significant decrease in the relative concentration of Ni and an appreciable increase in the relative concentration of Cr in the effluent. Thus, while the Ni in the effluent is now lower than the nominal value, Cr is appreciably higher than the nominal value for this alloy. This indicates that conditions now favor stable Ni. At this pH, as previously indicated,<sup>25</sup> these data suggest selective dissolution of chromium for oxidizing environments. Nevertheless, the measured total metal dissolution is significantly less (40 ppm after 15 h of exposure). The decreased corrosion rate results from the increase in the feed pH, altering the thermodynamic stability of Ni from soluble (Ni<sup>2+</sup>) to insoluble (NiO). Assuming that the experimentally indicated selective Cr depletion suggests HCrO<sub>4</sub><sup>-</sup> stability, it may be possible to decrease corrosion further by reducing the oxidizing potential of the feed to region 3 in Figure 3b.

**(c) Alkaline Chlorinated Feed (pH 12.7).** A further increase in pH results in data that again indicate selective dissolution of Cr. The total metal in the effluent has, however, decreased to a value 600 times lower than that recorded for the acidic feed (2.6 ppm after a 15 h). While this may be indicative of the potential for successful corrosion control by this methodology, longer term exposure experiments are needed.

The results presented in Figure 3 are particularly interesting because the behavior of the Inconel 625 alloy exposed to aqueous HCl was predicted quite accurately by the hypothesis developed during the failure analysis of a C-276 tube exposed to methylene chloride.<sup>25</sup> This suggests that such results not only may be valuable for specific alloys but also may be employed in a more general way to provide information on other alloys.

**Instrumented Tube Experiments.** To provide a more controlled assessment of the correlation between the temperature and corrosion rate, a number of experiments have been carried out in which an alloy C-276 tube was instrumented with thermocouples. These experiments were designed to correlate as closely as possible to conditions associated with the failure of the organic preheaters previously discussed. Because one of the major products of the hydrolysis of CH<sub>2</sub>Cl<sub>2</sub> occurring in the preheaters is hydrochloric acid, during the instrumented tube experiment, an aqueous HCl feed was introduced at a supercritical temperature and allowed to cool as it traversed the length of the tube. The ambient pHs of the feed and the effluent were both approximately 2. During previous work,<sup>31</sup> the following broad regions were delineated: (i) a region at high temperature in which no corrosion was identified, (ii) a transition zone at a somewhat lower temperature with some disconnected dealloying, (iii) a region in which a well-established dealloyed layer with little evidence of cracking was apparent. The thickness of this layer was inversely proportional to the measured temperature, exhibiting a tendency to thicken as the temperature decreased, (iv) a region in which both a dealloyed layer and intergranular cracking were observed. While the most severe cracking was associated with a subcritical temperature, the results were also interpreted to suggest the potential for crack development at higher temperatures during extended exposure.

While some temperature measurement problems were encountered during the previous experiment as a result

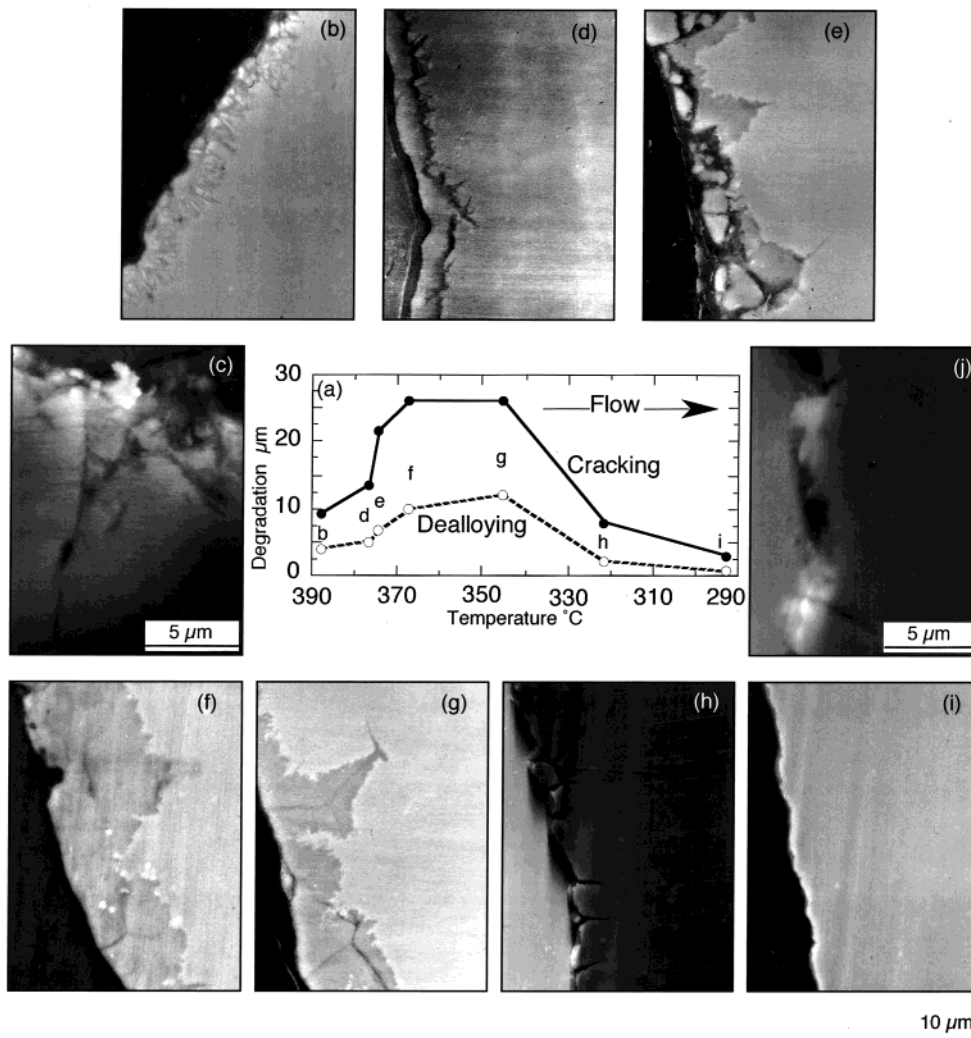


**Figure 4.** Results from an instrumented alloy C-276 tube as a function of temperature: (a) the extent of cracking and dealloying and (b–j) the appearance of the inner tube diameter. The tube was exposed to an HCl feed (pH  $\approx$  2) for a total test time of 19.5 h. Letters b and d–i within the graph refer to the corresponding micrograph. Micrographs c and j reveal a higher magnification of b and i, respectively.

of insufficient contact area between the tube and thermocouple, this problem was overcome in subsequent experiments by employing subminiature thermocouples.<sup>44</sup> Preliminary results are presented in Figure 4a–j.

Figure 4 presents the results for an alloy C-276 tube exposed to a 365 ppm aqueous HCl feed (pH  $\approx$  2) for a total test time of 19.5 h at a pressure of 24.6–25.3 MPa. Similar to results reported for the preheaters,<sup>31</sup> the depth of cracking and dealloying generally track each other closely (Figure 4a) as a function of temperature.

There is a distinct increase in degradation as the temperature decreases into the subcritical regime. The higher rate of degradation continues over a range of approximately 30 °C prior to decreasing again at approximately 345 °C. At the highest temperature assessed during this examination (Figure 4b), the morphology reflects disconnected dealloying similar to that reported previously.<sup>31</sup> At a higher magnification (Figure 4c), a crack was identified; however, it was not determined if the crack was preexisting or if it developed during the experiment. As the temperature approached the critical point (Figures 4d,e), the dealloying and cracking became well-established. Within this region the extent of cracking and dealloying tends to remain constant or increase slightly as the temperature is decreased (Figures 4f,g); however, below ap-

proximately 345 °C, the depth of penetration decreased significantly (Figure 4h). It is important to note, however, that while this region reflects a lower depth of penetration, it also reveals the maximum crack density. Finally, at a temperature of approximately 292.5 °C (Figure 4i), the degradation is minimal. One crack (which may have been preexisting) was located within this section (Figure 4j).

These results corroborate the hypothesis developed during the preheater failure analysis and initial instrumented tube experiment that maximum degradation for Ni-based alloys may be associated with high subcritical temperatures. However, this was a simple non-salt-forming feed and, in the presence of salt precipitates, corrosion behavior will change. Additionally, these were short-duration experiments, and cracking has been reported for Ni-based alloys, even at supercritical temperatures, after extended exposure.<sup>8</sup> Great care needs to be exercised, therefore, in extending these data to longer times or to systems where salts may develop.

**Exposure Studies.** Samples positioned within the top zone of the Modar reactor (Figure 1) were exposed for 66.2 h to a test temperature of approximately 600 °C in a highly chlorinated oxygenated organic feed stream containing C, H, O, N, Cl, S, Na, K, Si, and F, with small additions of Ce, Pb, and Zn. The materials



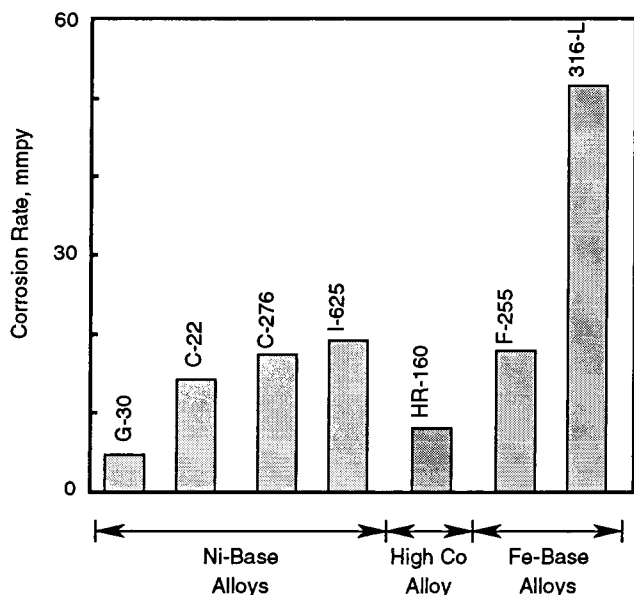


**Figure 5.** Mass loss data in millimeters per year (mmpy) for the various alloys exposed to an aggressive chlorinated SCWO feed stream.

chosen for testing included four Ni-based alloys (Inconel 625, Hastelloy C-276, C-22, and G-30), an austenitic stainless steel (316-L), a duplex stainless steel (Ferrarium 255) and a high-cobalt alloy (HR-160). Either nonwelded or welded and nonwelded coupons of each alloy were exposed and, in addition, U-bend samples of Inconel 625, Hastelloy C-276, and stainless steel type 316-L were included. Coupons were mounted on a titanium rod and insulated from the rod and each other by means of alumina spacers.

As indicated by the corrosion rate data (Figure 5), alloy G-30 reveals the best corrosion resistance and alloy HR-160 (high Co) also exhibits a good performance. The Ni-based alloys C-22, C-276, and I-625 exhibit comparable rates, while the Fe-based duplex steel (Ferrarium 255) reveals a rate similar to that of the Ni alloys. On the other hand, the austenitic stainless steel, 316-L, displayed the highest corrosion rate.

All samples were covered with both a salt layer and a black, tenacious oxide layer, which remained on the surface of the various samples even after removal of the salt layer by ultrasonic cleaning. Such salt deposits may be the precursors of severe corrosion<sup>36</sup> and have been linked to underdeposit corrosion of titanium.<sup>45</sup> Because the thickness of the oxide layer formed on alloys C-22, C-276, I-625, and 316-L also reflects increasing corrosion rates, it suggests the oxide layer does not provide any significant corrosion protection. Electron probe microanalysis for the various elements present within the oxide layer of the nickel alloys indicated nickel depletion in all cases.<sup>19</sup>

Both alloy C-276 and alloy I-625 exhibited pitting (Figure 6) and, in the case of C-276, some intergranular attack. Alloy C-22 revealed resistance superior to both alloy C-276 and I-625. For the conditions tested, alloy G-30 exhibited the best corrosion behavior.

## Summary and Conclusions

It is apparent that there is a region of the  $E$ -pH diagram where thermodynamic conditions favor the formation of insoluble Cr, Ni, and Fe at a high subcritical temperature (300 °C). Maintaining this region by

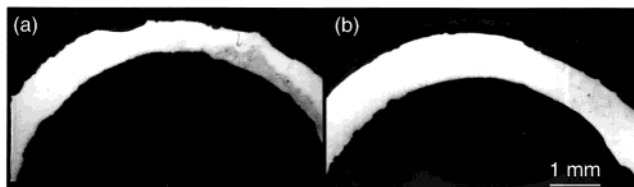


**Figure 6.** Cross section of (a) alloy C-276 and (b) I-625 after exposure to a highly chlorinated SCWO feed stream.

feed chemistry control during waste destruction may reduce degradation.

Test results corroborate the strong correlation between the feed pH and the relative dissolution of Ni and Cr for Ni-based alloys. Acidic conditions tend to favor Ni dissolution and basic conditions tend toward Cr dissolution.

During the failure analysis, it was recognized that corrosion was minimized within known supercritical regions and cracking was, therefore, assumed to develop preferentially within a high subcritical regime. This was corroborated by subsequent instrumented tube experiments designed to closely reflect conditions associated with the preheaters. These data were, however, for short-duration experiments and a simple non-salt-forming feed. Because cracking of Ni-based alloys has been reported<sup>8</sup> at supercritical temperatures after extended exposure, great care needs to be exercised in extending these data to longer times or to systems where salts may develop.

## Literature Cited

- (1) The NATO Advanced Workshop, Destruction of Military Toxic Waste, Naaldwijk, The Netherlands, May 22–27, 1994; U.S. Army Research Office Report.
- (2) Drake, L. Selecting Technologies for Destruction of the Chemical Weapons Stockpile. MIT Energy Laboratory Seminar, Massachusetts Institute of Technology, Cambridge, MA, Feb 9, 1993.
- (3) *Aqua fortis*, U.S. Army Research Office **1993**, 2 (No. 2).
- (4) *Aqua fortis*, U.S. Army Research Office **1994**, 3 (No. 1).
- (5) *Aqua fortis*, U.S. Army Research Office **1993**, 2 (No. 1).
- (6) Swallow, K. C.; Ham, D. *Nucleus* **1993**, 11, 11.
- (7) Downey, K. W.; Snow, R. H.; Hazlebeck, D. A.; Roberts, A. J. *Science and Technology*; ACS Symposium Series 608; American Chemical Society: Washington, DC, 1995; p 313.
- (8) Latanision, R. M., Shaw, R. W. Co-Chairs. Corrosion in Supercritical Water Oxidation Systems. Summary of a Workshop held at Massachusetts Institute of Technology, May 6 and 7, 1993; Report No. MIT-EL 93-006.
- (9) Mitton, D. B.; Orzalli, J. C.; Latanision, R. M. *Proc. 3rd Int. Symp. Supercrit. Fluids* **1994**, 3, 43.
- (10) Thomas, A. J.; Gloyne, E. F. *Corrosion Behavior of High Grade Alloys in the Supercritical Water Oxidation of Sludges*; Technical Report CRWR 229; University of Texas at Austin: Austin, TX, 1991.
- (11) Tester, J. W.; Holgate, H. R.; Armellini, F. J.; Webley, P. A.; Killilea, W. R.; Hong, G. T.; Barner, H. E. *Emerging Technologies for Waste Management III*; ACS Symposium Series 518; American Chemical Society: Washington, DC, 1993; p 35.
- (12) Modell, M. *Standard Handbook of Hazardous Waste Treatment and Disposal*; McGraw-Hill: New York, 1989.
- (13) Franck, E. U. *High Temperature, High-Pressure Electrochemistry in Aqueous Solutions*; NACE: Houston, TX, 1976.
- (14) LaJeunesse, C. A.; Mills, B. E.; Brown, B. G. *Supercritical Water Oxidation of Ammonium Picrate*; Sandia Report SAND95-8202-UC-706; Sandia National Laboratories: Albuquerque, NM, 1994.
- (15) Tebbal, S.; Kane, R. D. *Corrosion 98*; NACE: Houston, TX, 1998; Paper 413.
- (16) Boukis, N.; Landvatter, R.; Habicht, W.; Franz, G. First Experimental SCWO Corrosion Results of Ni-Base Alloys Fabricated as Pressure Tubes and Exposed to Oxygen Containing

Diluted Hydrochloric Acid at  $\leq 450$  °C,  $P = 24$  MPa. First International Workshop on Supercritical Water Oxidation, Jacksonville, FL, 1995.

(17) Mitton, D. B.; Orzalli, J. C.; Latanision, R. M. *12th ICPWS*; Begell House: New York, 1995; p 638.

(18) Mitton, D. B.; Zhang, S.-H.; Han, E.-H.; Hautanen, K. E.; Latanision, R. M. Proceedings of the 13th ICC, Melbourne, Australia, 1996.

(19) Mitton, D. B.; Kim, Y. S.; Yoon, J. H.; Take, S.; Latanision, R. M. *Corrosion 99*; NACE: Houston, TX, 1999; Paper 257.

(20) Konys, J.; Fodi, S.; Ruck, A.; Hausselt, J. *Corrosion 99*; NACE: Houston, TX, 1999; Paper 253.

(21) ASM Handbook. *Corrosion*, 9th ed.; ASM International: Materials Park, OH, 1987; Vol. 13, p 641.

(22) Orzalli, J. C. Preliminary Corrosion Studies of Candidate Materials for Supercritical Water Oxidation Reactor Systems. Master's Thesis, Department of Materials Science and Engineering, Massachusetts Institute of Technology, Cambridge, MA, 1994.

(23) Norby, B. C. *Supercritical Water Oxidation Benchscale Testing Metallurgical Analysis Report*; Report EGG-WTD-10675; Idaho National Engineering Laboratory; Idaho Falls: ID, 1993.

(24) Latanision, R. M. *Corrosion* **1995**, 51 (4), 270.

(25) Mitton, D. B.; Marrone P. A.; Latanision, R. M. *J. Electrochem. Soc.* **1996**, 143, L59.

(26) Mitton, D. B.; Orzalli, J. C.; Latanision, R. M. *Science and Technology*; ACS Symposium Series 608; American Chemical Society: Washington, DC, 1995; p 327.

(27) Kane, R. D.; Cuellar, D. *Literature and Experience Survey on Supercritical Water Corrosion*; CLI International Report No. L941079K; CLI; Houston, TX, 1994.

(28) Wozaldo, G. P.; Pearl, W. L. *Corrosion* **1965**, 21, 355.

(29) Bramlette, T. T.; Mills, B. E.; Hencken, K. R.; Brynildson, M. E.; Johnston, S. C.; Hruby, J. M.; Feemster, H. C.; Odegard, B. C.; Modell, M. *Destruction of DOE/DP Surrogate Wastes with Supercritical Water Oxidation Technology*; Sandia National Laboratories Report SAND90-8229; Sandia National Laboratories: Albuquerque, NM, 1990.

(30) Rice, S. F.; Steeper, R. R.; LaJeunesse, C. A. *Destruction of Representative Navy Wastes Using Supercritical Water Oxidation*; Sandia Report SAND94-8203 UC-402; Sandia National Laboratories: Albuquerque, NM, 1993.

(31) Mitton, D. B.; Zhang, S.-H.; Quintana, M. S.; Cline, J. A.; Caputy, N.; Marrone, P. A.; Latanision, R. M. *Corrosion 98*; NACE: Houston, TX, 1998; Paper 414.

(32) Hong, G. T.; Ordway, D. W.; Ziberstein, V. A. Materials Testing in Supercritical Water Oxidation Systems. First Interna-

tional Workshop on Supercritical Water Oxidation, Jacksonville, FL, 1995.

(33) Kritzer, P.; Boukis, N.; Dinjus, E. *Corrosion 98*; NACE: Houston, TX, 1998; Paper 414.

(34) Huang, S.; Daehling, K.; Carleson, T. E.; Abdel-latif, M.; Taylor, P.; Wai, C.; Propp, A. Electrochemical Measurement of Corrosion of Iron Alloys in Supercritical Water. *Supercritical Fluid Science and Technology*; ACS Symposium Series 406; American Chemical Society: Washington, DC, 1989; p 287.

(35) Kriksunov, L. B.; Macdonald, D. D. *J. Electrochem. Soc.* **1995**, 4069.

(36) Garcia, K. M.; Mizia, R. Corrosion Investigation of Multilayered Ceramics and Experimental Nickel Alloys in SCWO Process Environments. First International Workshop on Supercritical Water Oxidation, Jacksonville, FL, 1995.

(37) Fodi, S.; Konys, J.; Hausselt, J.; Schmidt, H.; Casal, V. *Corrosion 98*; NACE: Houston, TX, 1998; Paper 416.

(38) Barnes, C. M.; Marshall, R. W.; Mizia, R. E.; Herring, J. S.; Peterson, E. S. *Identification of Technical Constraints for Treatment of DOE Mixed Waste by Supercritical Water Oxidation*; Idaho National Engineering Laboratory: Idaho Falls, ID, 1993; EGG-WTD-10768.

(39) Hong, G. T. (MODAR). Personal communication, 1997.

(40) Fassbender, A. G.; Robertus, R. J.; Daverman, G. S. The Dual Shell Pressure Balanced Vessel: A Reactor for Corrosive Applications. First International Workshop on Supercritical Water Oxidation, Jacksonville, FL, 1995.

(41) LaRoche, H. L.; Weber, M.; Trepp, Ch. Rationale for the Filmcooled Coaxial Hydrothermal Burner (FCHB) for Supercritical Water Oxidation (SCWO). First International Workshop on Supercritical Water Oxidation, Jacksonville, FL, 1995.

(42) Weber, M.; Wellig, B.; von Rohr, R. *Corrosion 99*; NACE: Houston, TX, 1999; Paper 258.

(43) Kritzer, P.; Boukis, N.; Dinjus, E. *Corrosion* **1998**, 54, 824.

(44) Cline, J. A. Experimental and Ab Initio Investigations of Corrosion in Supercritical Water Oxidation Systems. Ph.D. Dissertation, Massachusetts Institute of Technology, Cambridge, MA, 2000.

(45) Garcia, K. M. *Supercritical Water Oxidation Data Acquisition Testing*; INEL Report INEL-96/0267; INEL: Idaho Falls, ID, 1996.

Received for review February 1, 2000  
Revised manuscript received August 9, 2000  
Accepted August 15, 2000

IE000124K